Electronic Supporting Information (ESI)

Mono-substituted cage-like silsesquioxanes bound by trifunctional acyl chloride as multi-donor N,O-type ligand in copper(II) coordination chemistry: synthesis and structural properties

Kamila Piec[a], Joanna Wątły[a], Maria Jerzykiewicz[a], Julia Kłak[a], Andrzej Plichta[b] and Łukasz John[a,*]

[a]*Faculty of Chemistry, University of Wrocław, 14 F. Joliot-Curie, 50-383, Wrocław, Poland*
[b]*Faculty of Chemistry, Warsaw University of Technology, 3 Noakowskiego, 00-664 Warsaw, Poland*

Corresponding author: Dr. Łukasz John, D.Sc. e-mail: lukasz.john@chem.uni.wroc.pl

Table of Contents

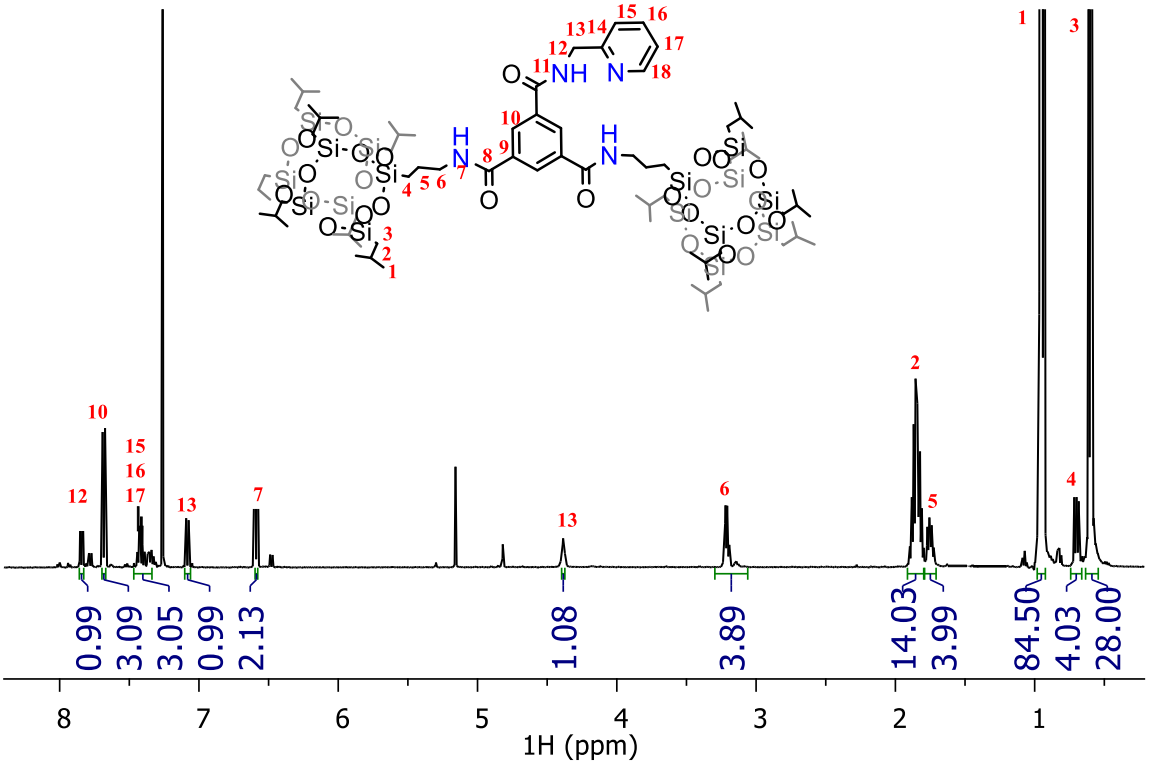

Figure S1. ^{1}H NMR (500 MHz, $CDCl_3$, 300 K) spectrum of **POSS-1**.

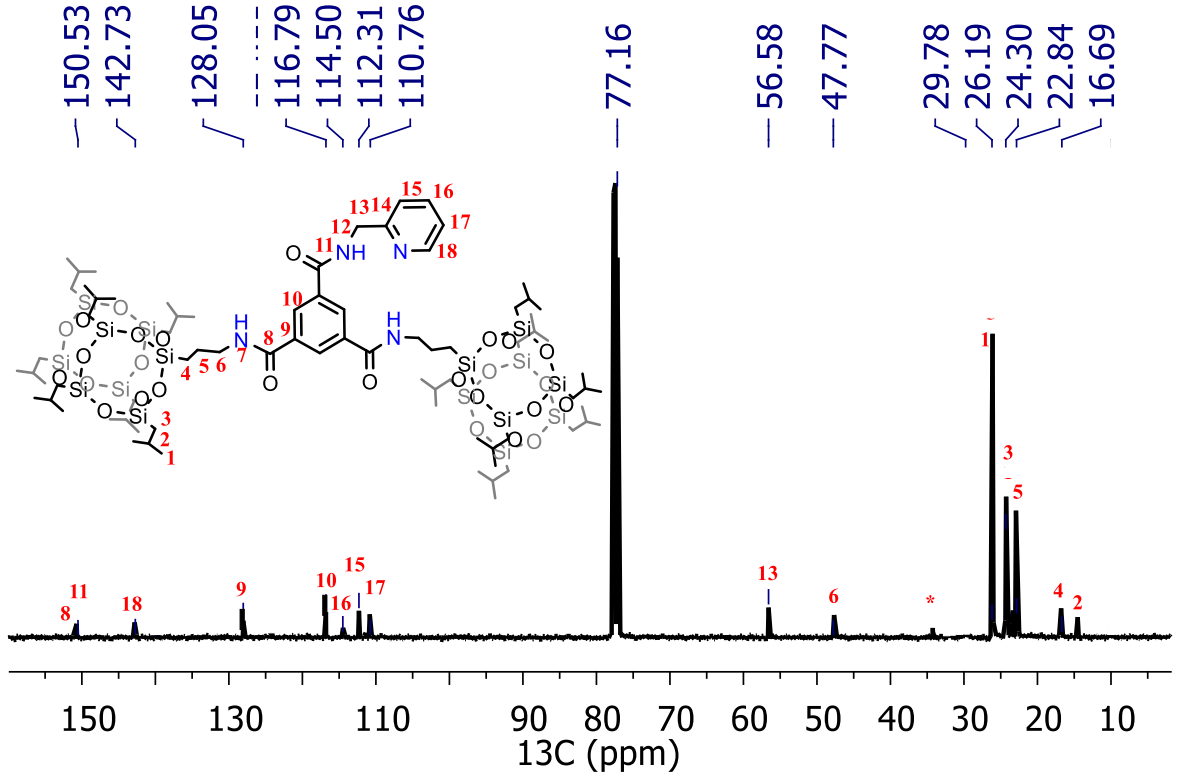

Figure S2. ^{13}C NMR (126 MHz, $CDCl_3$, 300 K) spectrum of **POSS-1**.

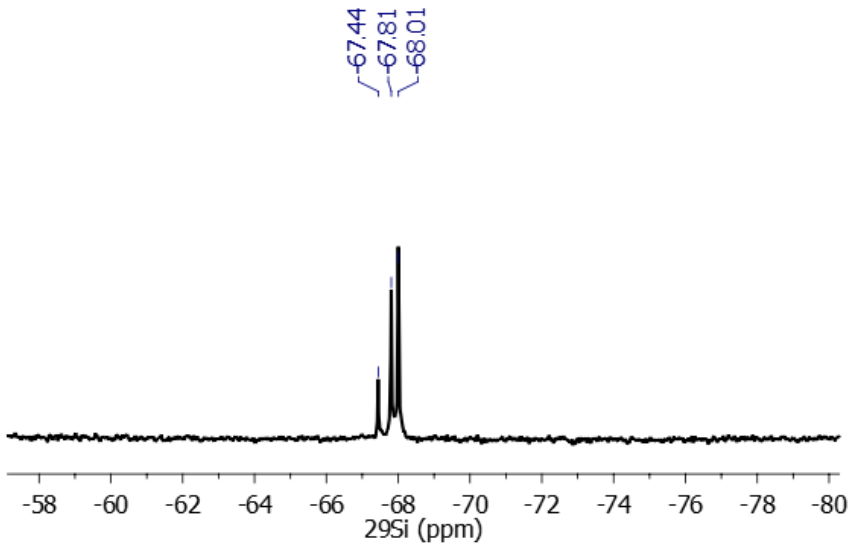

Figure S3. ^{29}Si NMR (59.6 MHz, $CDCl_3$, 300 K) spectrum of **POSS-1**.

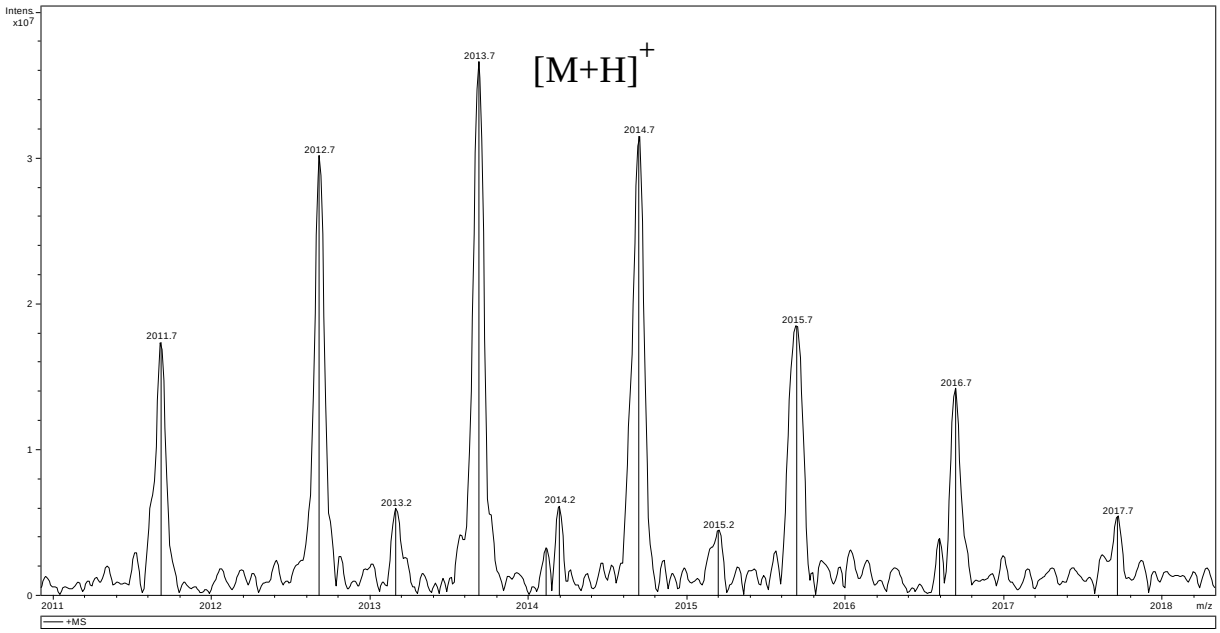

Figure S4. HR-MS (ESI^+, TOF, $CHCl_3$) spectrum of **POSS-1**.

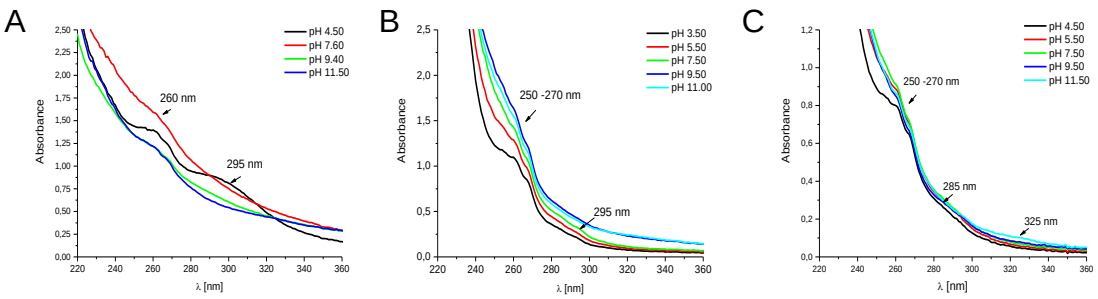

Figure S5. Solution absorption spectra of **Cu-X/POSS-1** complexes (X = 1, 2, 3 for A, B, and C, respectively) at UV region at different pH values. Complexes were solubilized in ethanol at 298 K.

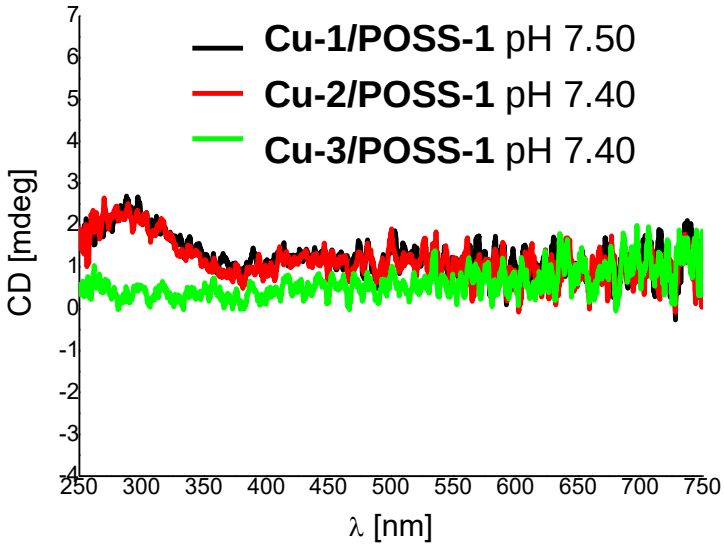

Figure S6. CD spectra of **Cu-1/POSS-1**, **Cu-2/POSS-1** and **Cu-3/POSS-1**.

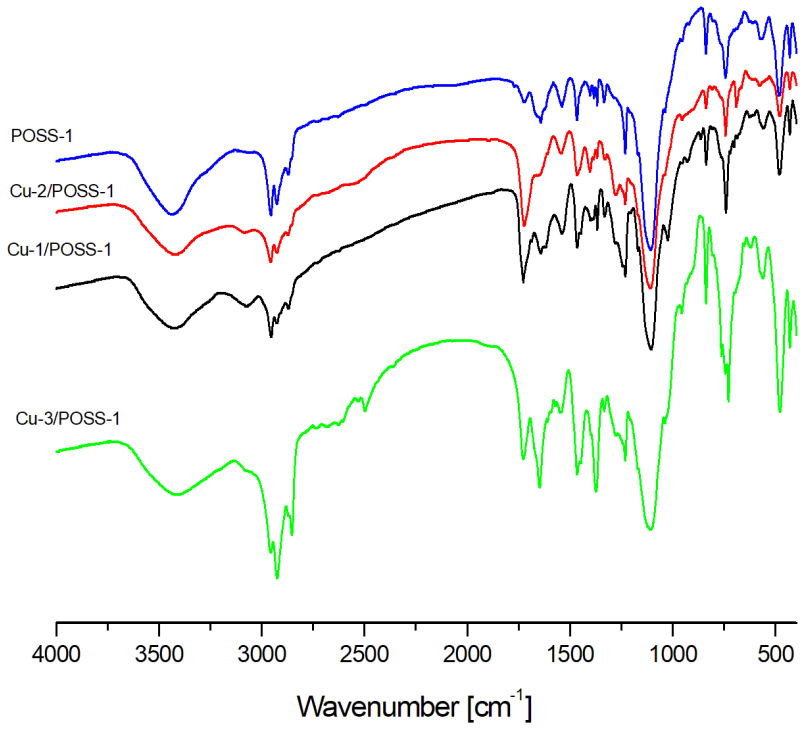

Figure S7. FT-IR (KBr pellets) spectra of **POSS-1**, **Cu-1@POSS-1**, **Cu-2@POSS-1**, and **Cu-3@POSS-1**.

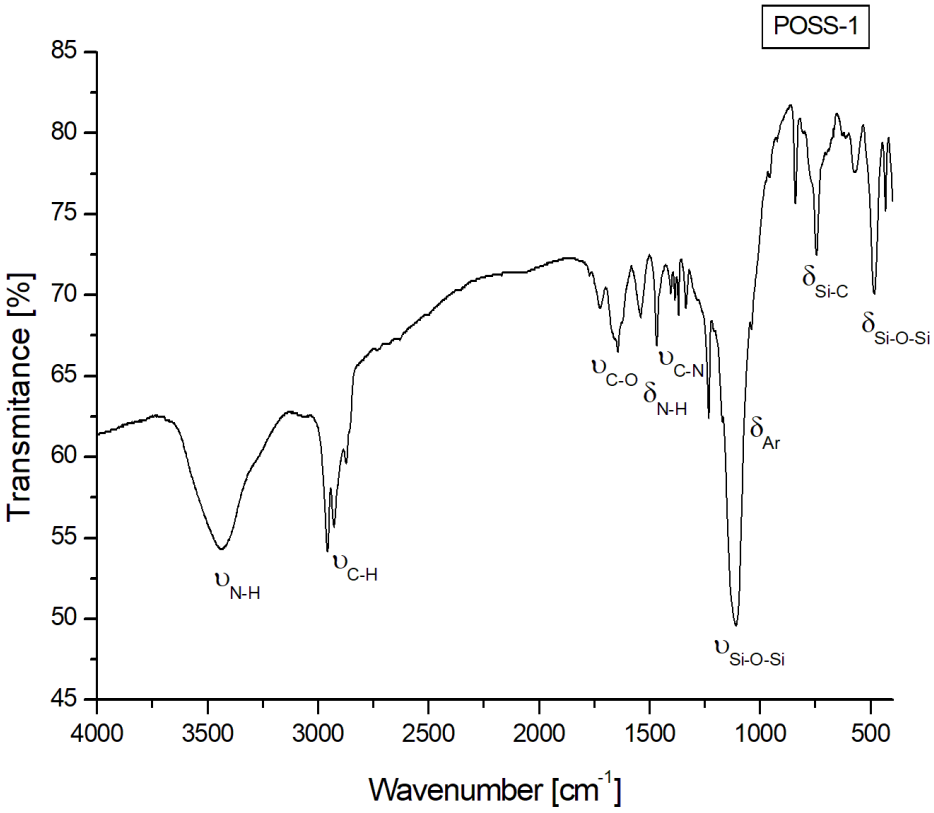

Figure S8. FT-IR (KBr pellets) spectrum of **POSS-1**.

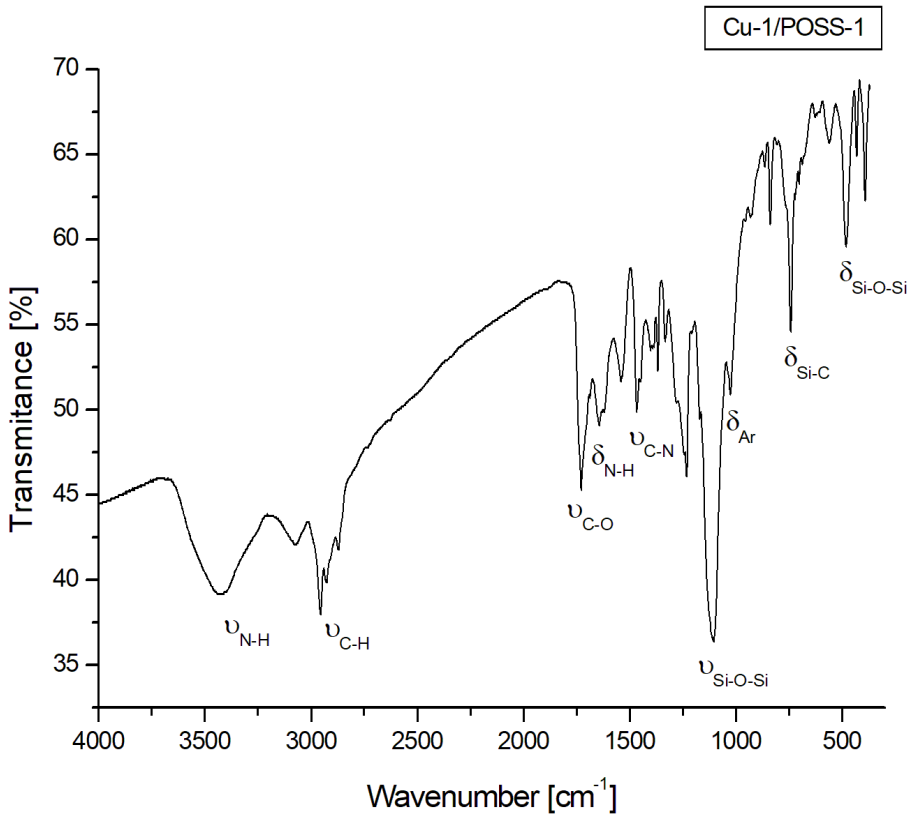

Figure S9. FT-IR (KBr pellets) spectrum of **Cu-1/POSS-1**.

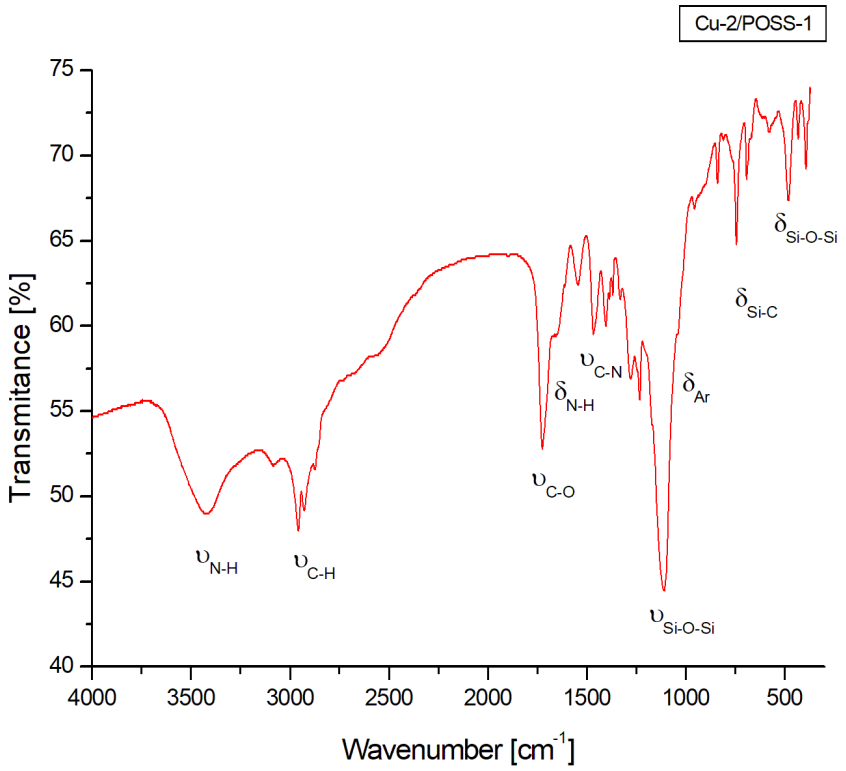

Figure S10. FT-IR (KBr pellets) spectrum of **Cu-2/POSS-1**.

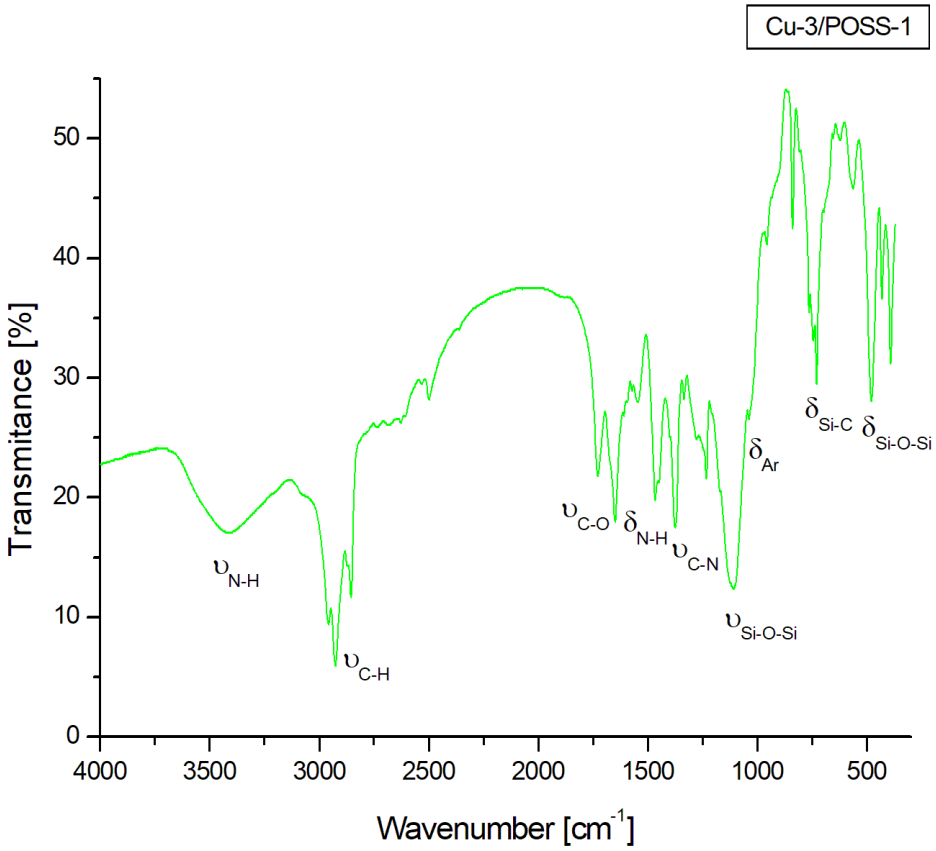

Figure S11. FT-IR (KBr pellets) spectrum of **Cu-3/POSS-1**.

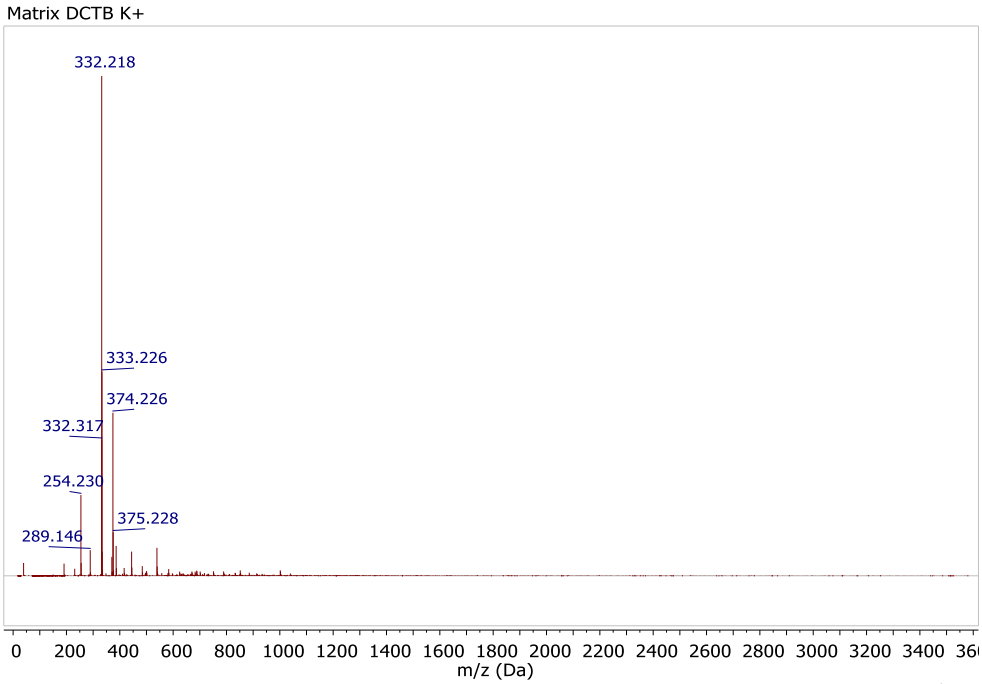

Figure S12. MALDI ToF mass spectrum of DCTB matrix enriched with K^+ ions (range of 0 – 3600 m/z).

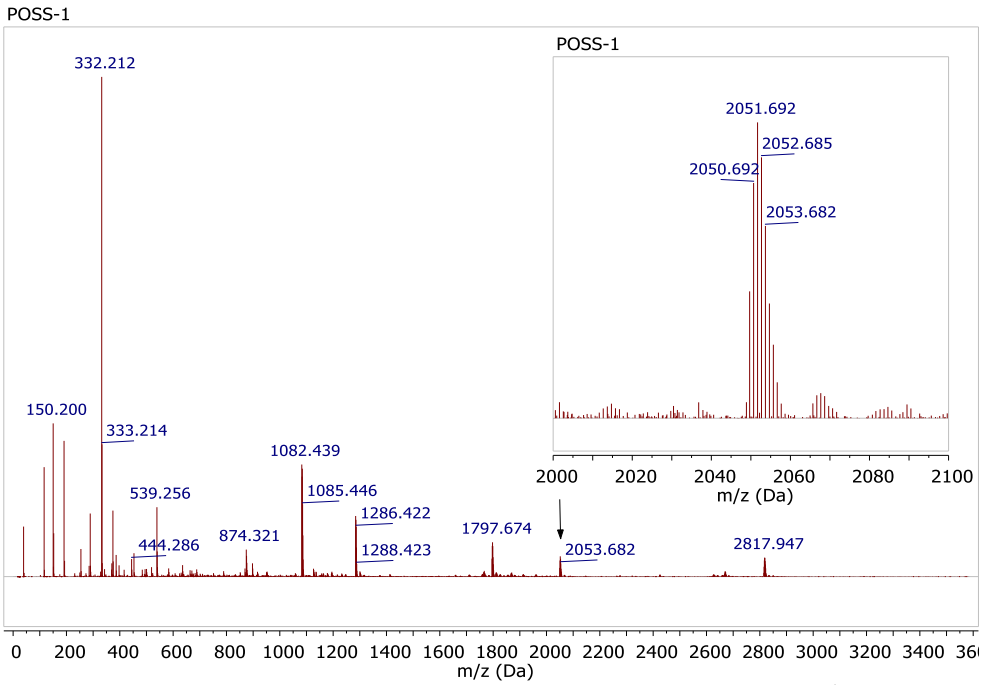

Figure S13. MALDI ToF mass spectrum of **POSS-1** enriched with K^+ ions (full range of 0 – 3600 m/z and inset of 2000 – 2100 m/z).

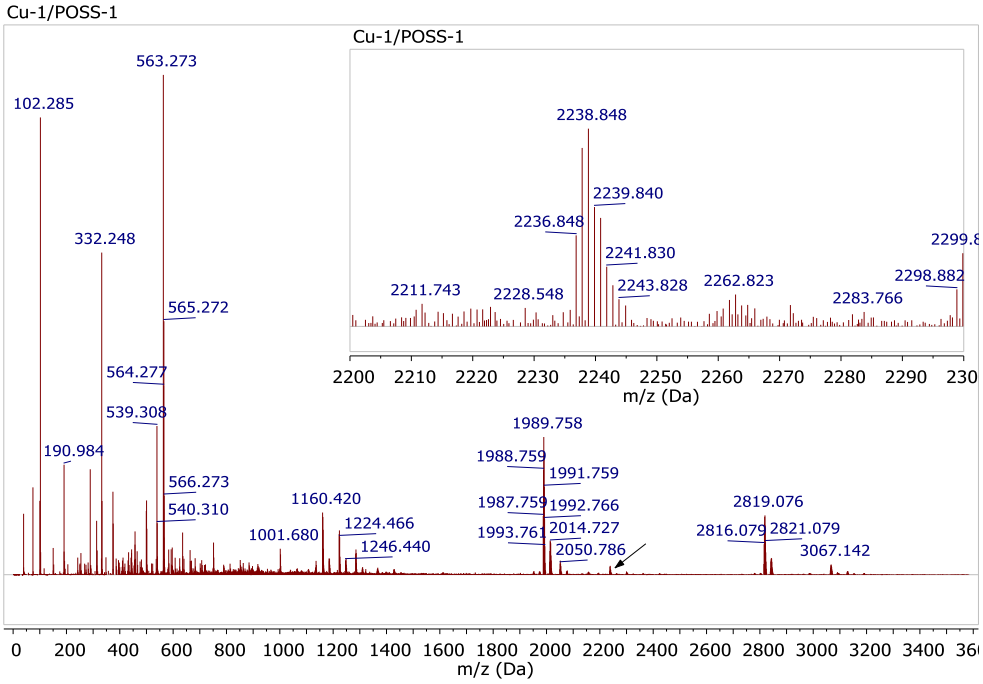

Figure S14. MALDI ToF mass spectrum of **Cu-1/POSS-1** enriched with K^+ ions (full range of 0 – 3600 m/z and inset of 2200 – 2300 m/z).

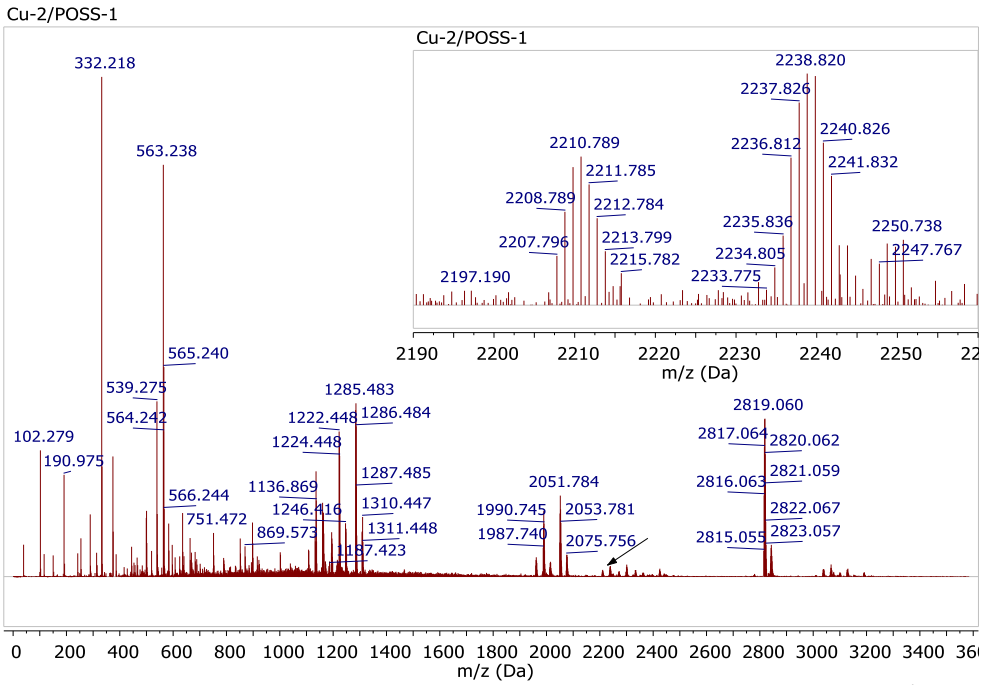

Figure S15. MALDI ToF mass spectrum of **Cu-2/POSS-1** enriched with K^+ ions (full range of 0 – 3600 m/z and inset of 2190 – 2260 m/z).

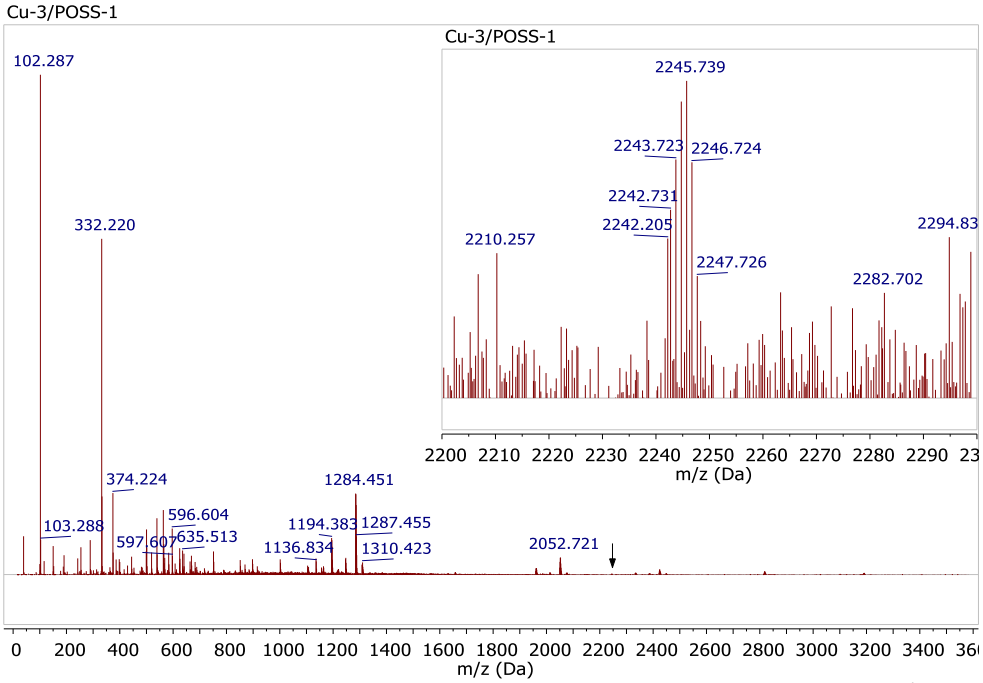

Figure S16. MALDI ToF mass spectrum of **Cu-3/POSS-1** enriched with K^+ ions (full range of 0 – 3600 m/z and inset of 2200 – 2300 m/z).

Table S1. Thermal properties of **POSS-1, Cu-1/POSS-1, Cu-2/POSS-1** and **Cu-3/POSS-1** based on TG-DTA studies.

Comp.	Atm.	Melting temperature [°C]	Calculated residue yield [%]	Residue yield [%]	Δ	$T_{5\%}$	T_1	T_2	T_3
POSS-1	Air	87	47.75	23.87	23.88	198	282	394	-
POSS-1	N_2	87	47.75	19.87	27.88	127	310	581	-
Cu-1/POSS-1	Air	78	46.30	27.44	18,86	151	210	248	482
Cu-1/POSS-1	N_2	78	46.30	6.84	39.46	172	275	570	-
Cu-2/POSS-1	Air	92	46.30	31.53	14.77	142	268	490	-
Cu-2/POSS-1	N_2	92	46.30	28.56	17.74	180	210	340	-
Cu-3/POSS-1	Air	80	46.30	34.30	12.00	212	284	605	-
Cu-3/POSS-1	N_2	80	46.30	11.34	34.96	198	261	302	622

Note: Calculated residue yield [%] calculated based on the decomposition to silicon dioxide SiO_2. Δ = The difference between the determined and calculated values. $T_{5\%}$ refers to the temperature at which a 5% loss in weight is observed. The T_1, T_2, T_3 temperatures correspond to the maximum rate of decomposition for each stage evaluated from the peaks of the DTG curves.

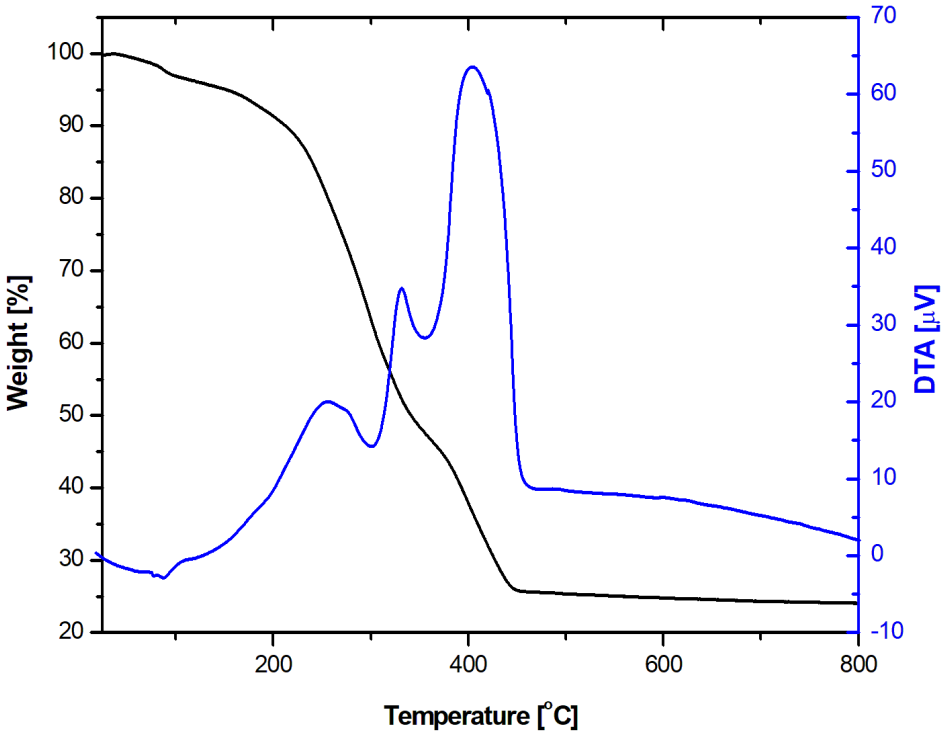

Figure S17. TG (black line), and DTA (blue line) thermogram of **POSS-1** at a heating rate of 5 °C/min. In the air atmosphere (60% N_2, 40% O_2).

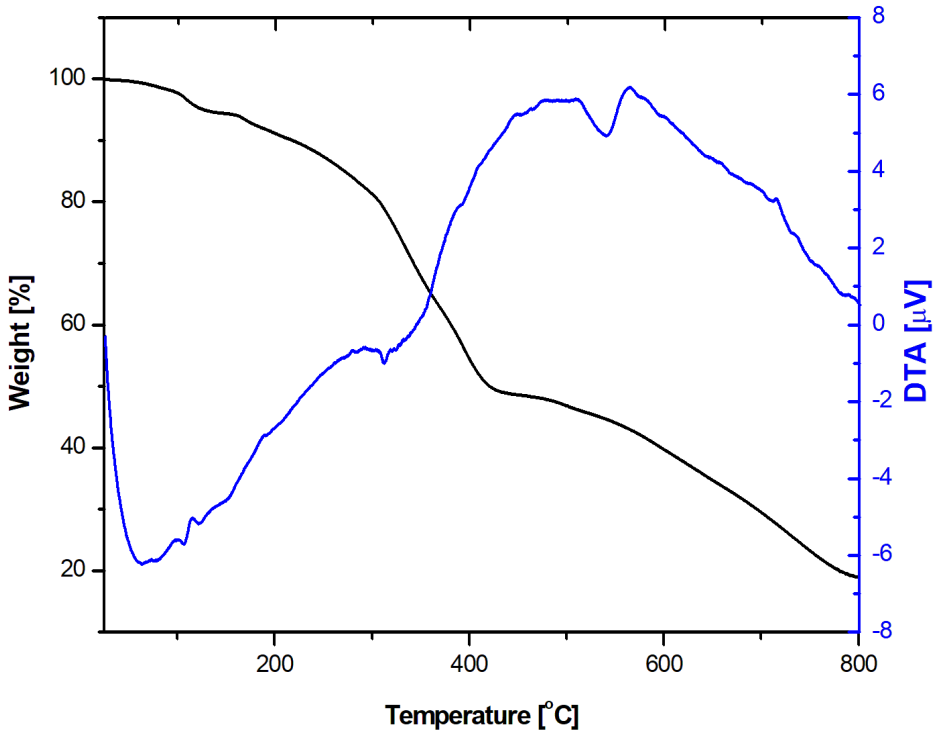

Figure S18. TG (black line), and DTA (blue line) thermogram of **POSS-1** at a heating rate of 5 °C/min. In the nitrogen.

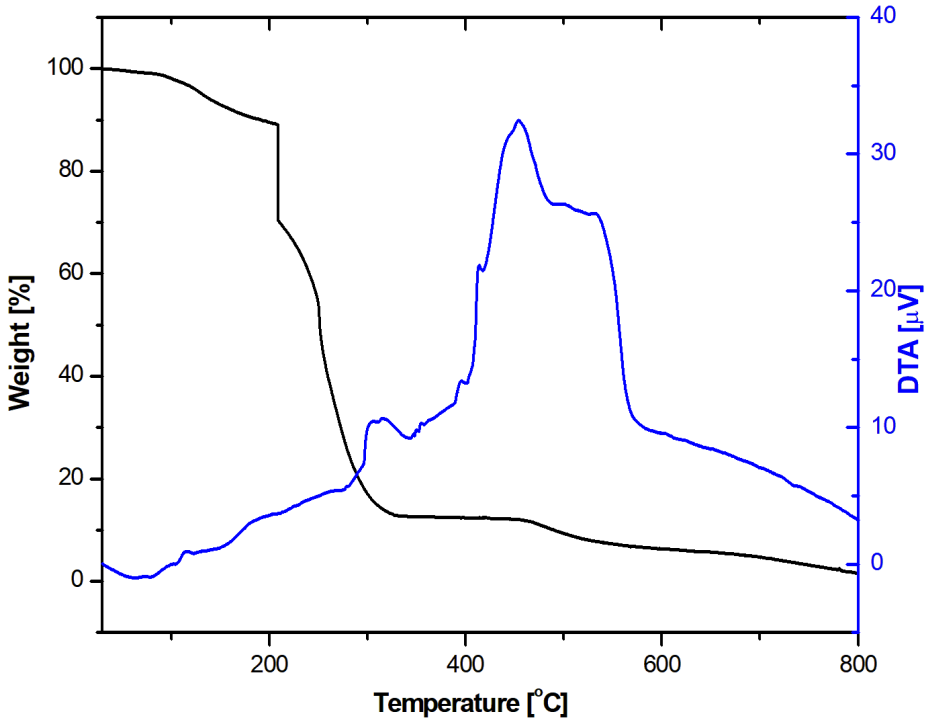

Figure S19. TG (black line), and DTA (blue line) thermogram of **Cu-1/POSS-1** at a heating rate of 5 °C/min. In the air atmosphere (60% N_2, 40% O_2).

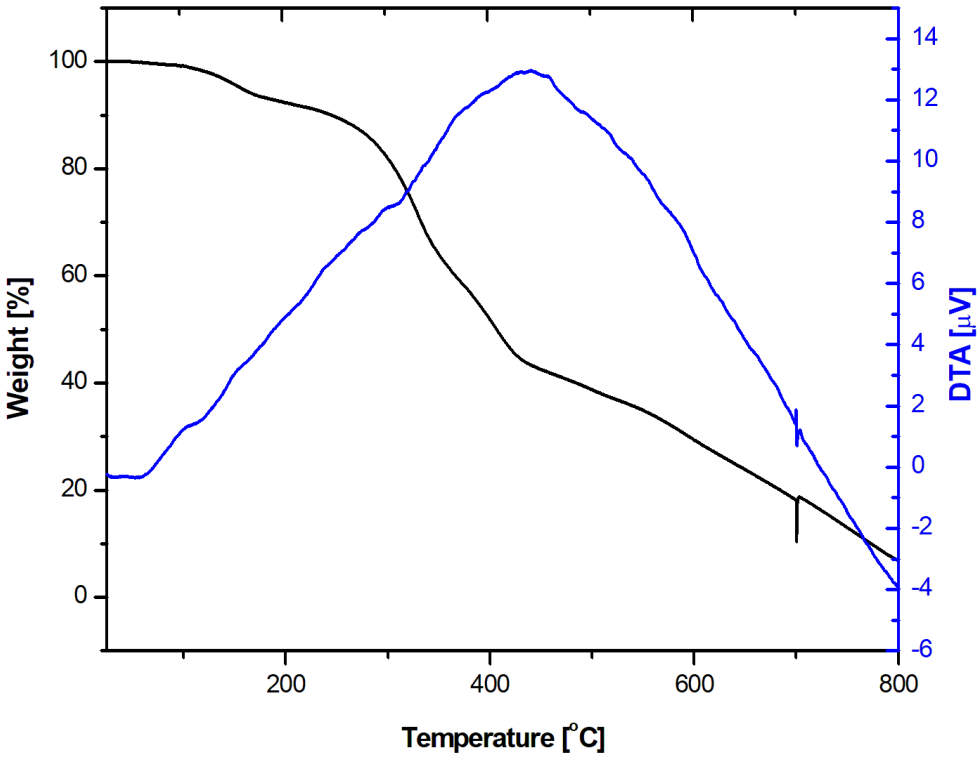

Figure S20. TG (black line), and DTA (blue line) thermogram of **Cu-1/POSS-1** at a heating rate of 5 °C/min. In the nitrogen.

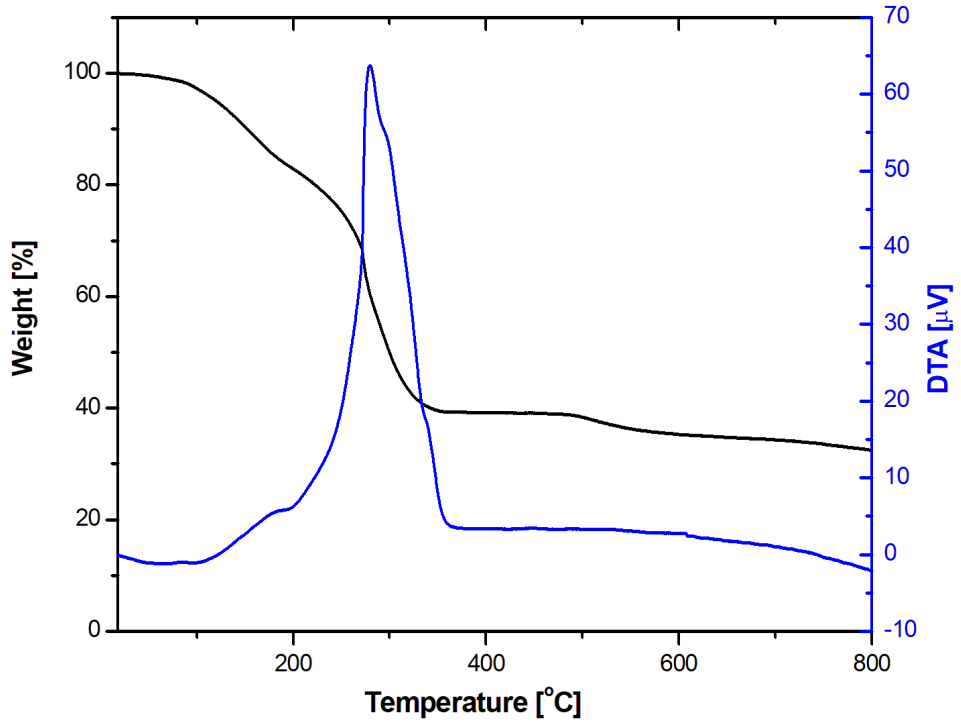

Figure S21. TG (black line), and DTA (blue line) thermogram of **Cu-2/POSS-1** at a heating rate of 5 °C/min. In the air atmosphere (60% N_2, 40% O_2).

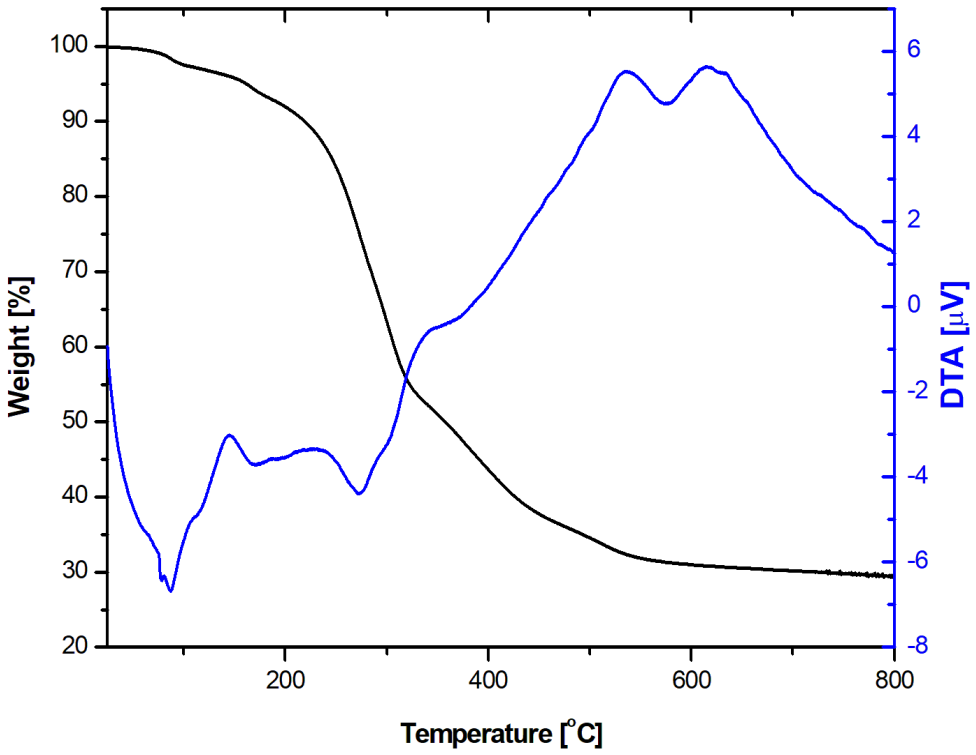

Figure S22. TG (black line), and DTA (blue line) thermogram of **Cu-2/POSS-1** at a heating rate of 5 °C/min. In the nitrogen.

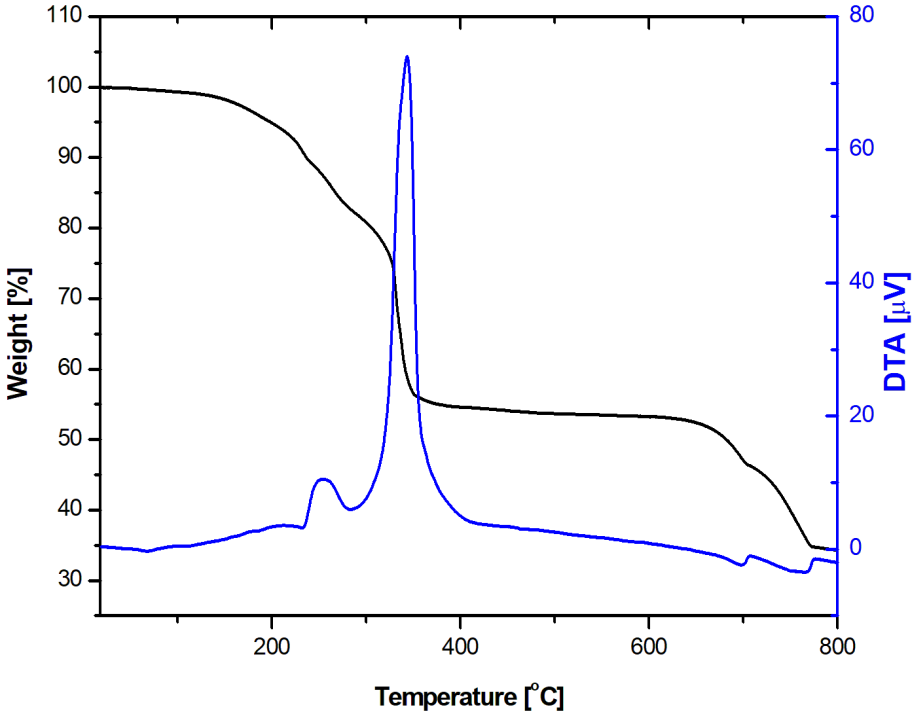

Figure S23. TG (black line), and DTA (blue line) thermogram of **Cu-3/POSS-1** at a heating rate of 5 °C/min. In the air atmosphere (60% N_2, 40% O_2).

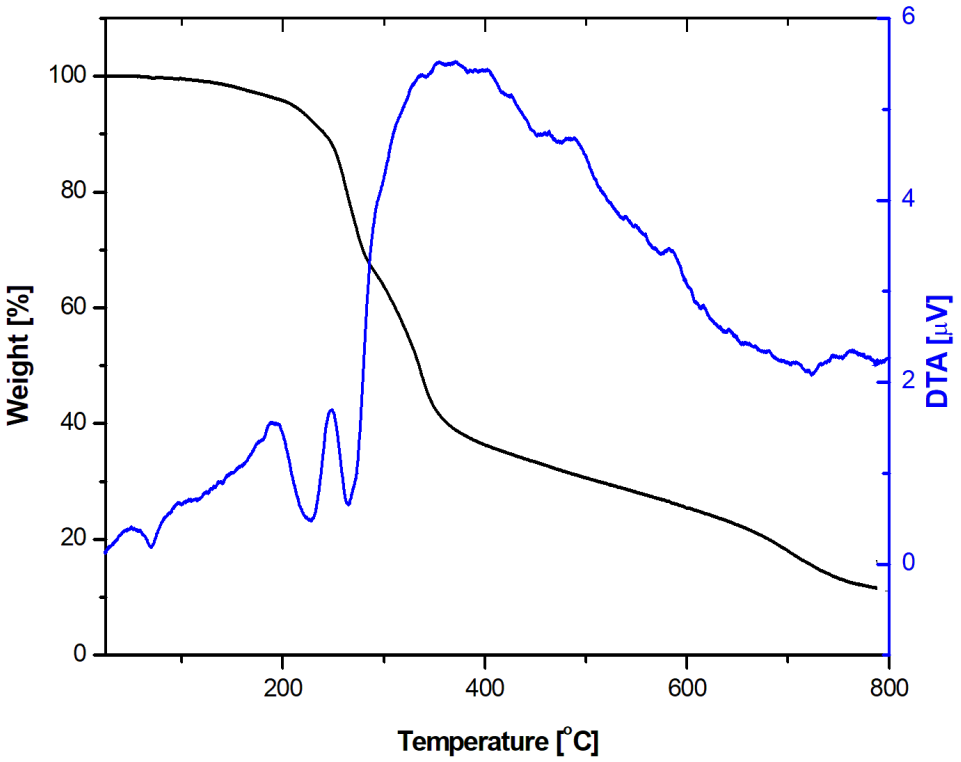

Figure S24. TG (black line), and DTA (blue line) thermogram of **Cu-3/POSS-1** at a heating rate of 5 °C/min. In the nitrogen.

Appendix. Preliminary catalytic studies.

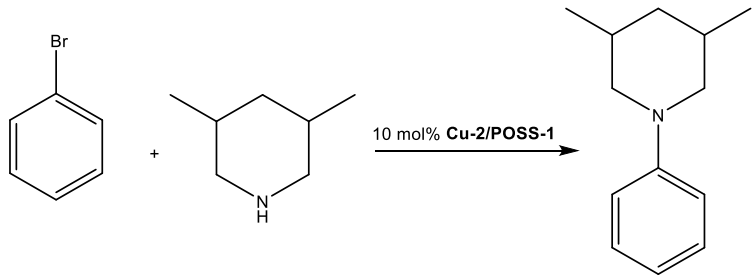

Schlenk flask was charged with bromobenzene (0.0785 g, 0.5 mmol), piperidine (0.679 g, 0.6 mmol), K_2CO_3 (0.276g, 2.0 mmol), and **Cu-2/POSS**-1 powder (0.0208 g, 0.01 mmol) dissolved in solvent (20 mL). The resulting mixture was vigorously stirred at 120 ^oC (in DMSO) or reflux (in CH_2Cl_2) for 24 h. After this time, clear solution was cooled to RT. Product was filtered by silica gel and dried under vacuum. As the base in the catalytic reactions, instead of K_2CO_3, also Et_3N (0.276 g, 2.0 mmol) and $(CH_3)_3CONa$ (0.112 g, 2.0 mmol) were used. The reagent conversions and product yields were monitored by GC-MS analyses.

Base (mmol)	Solvent (mmol)	Temperature (^oC)	Time (h)	Yield (%)
K_2CO_3 (2.0)	DMSO	120	24	0
K_2CO_3 (2.0)	CH_2Cl_2	reflux	24	0
Et_3N (2.0)	DMSO	120	24	5
Et_3N (2.0)	CH_2Cl_2	reflux	24	11
$(CH_3)_3CONa$ (2.0)	DMSO	120	24	14
$(CH_3)_3CONa$ (2.0)	CH_2Cl_2	reflux	24	26

References

1. H. Shargi, M. Aberi and P. Shiri, *Appl. Organometal. Chem.*, 2017, **31**, e3761.
2. F. Du, Q. Zhou, Y. Fu, Y. Chen, Y. Wu and G. Chen, Synlett., 2019, **30**, A-H.